CHAPTER

1 Autism spectrum disorders: Unbiased functional connectomics provide new insights into a multifaceted neurodevelopmental disorder

Archana Venkataraman

Department of Electrical and Computer Engineering, Johns Hopkins University, Baltimore, MD, United States

CHAPTER OUTLINE

INTRODUCTION

Autism spectrum disorder (ASD) affects an estimated 1 in 68 children in the United States, often with devastating effects on both patients and family members (Centers for for Disease Control, 2012; Leslie and Martin, 2007; Stuart and McGrew, 2009). From a neuroscientific perspective, ASD cannot be viewed as a single unified brain dysfunction (Aoki et al., 2013; Waterhouse and Gilberg, 2014); rather, it manifests through a series of distributed interactions across the brain (Cherkassky et al., 2006; Geschwind and Konopka, 2009; Sullivan et al., 2014). Behaviorally, ASD is characterized by blunted sociocommunicative skill and awareness across multiple sensory domains (Kanner, 1943; Pelphrey et al., 2014), coupled with stereotyped patterns

Connectomics. https://doi.org/10.1016/B978-0-12-813838-0.00001-7

of behaviors (Americal Psychiatric Association, 2013). However, the manifestation and severity of these clinical symptoms vary considerably across individuals and over the lifespan of each patient. In short, ASD is a complex and multifaceted disorder, and despite ongoing efforts, we have a limited understanding of its origin and pathogenesis. (Gabrieli-Whitfield et al., 2009; Hernandez et al., 2015; Sullivan et al., 2014).

Among its diverse behavioral presentations, social and language dysfunctions are considered hallmark and unifying features of ASD (Baron-Cohen et al., 1999; Kanner, 1943; Pelphrey et al., 2014). Social impairments are apparent in both verbal and nonverbal domains, and they manifest across simple (e.g., shared gaze) and complex (e.g., back-and-forth conversation) behaviors. On the language side, patients with ASD have notable difficulties with the production and interpretation of human speech (Globerson et al., 2015; Grossman et al., 2010). Because these deficits emerge within the first years of life, one popular theory in the field suggests that ASD alters both the structural and functional development of the brain via experience-dependent processes (Courchesne and Pierce, 2005; Geschwind and Levitt, 2007; Just et al., 2012; Melillo and Leisman, 2011). Functional magnetic resonance imaging (fMRI) is one of the most popular tools for studying neurological changes in ASD. For example, an investigation of speech processing in sleeping 2- to 3-year-old children found reduced activity in brain regions associated with language comprehension (Redcay and Courchesne, 2008). Likewise, a study of verbal fluency found atypical hemispheric lateralization in ASD (Kleinhans et al., 2008). Other fMRI studies have revealed significant changes in neural activity related to reward processing (Scott-Van Zeeland et al., 2010; Schmitz et al., 2008), joint attention (Belmonte and Yurgelun-Todd, 2003; Williams et al., 2005), and working memory (Koshino et al., 2005, 2008). Although valuable, it is worth emphasizing that these paradigms are designed to trigger specific neural activation using a narrow range of experimental stimuli. For this reason, one can argue that task fMRI studies do not capture naturalistic and whole-brain interactions.

This book chapter highlights the promise of functional connectomics in the study of ASD. Unlike task-based paradigms, functional connectomics allows us to quantify the synchrony between brain regions at both local and long-range scales. This flexibility offers a holistic perspective of ASD across multiple brain systems. Likewise, the absence of external stimuli allows us to focus on intrinsic or steady-state communication patterns. "Functional Connectomics as a Window into ASD" section of this chapter summarizes prior work in the field, from simple seed-based analyses to more complex network models. "An Unbiased Bayesian Framework for Functional Connectomics" section introduces our novel Bayesian framework to extract the altered subnetworks associated with ASD. In "Multisite Network Analysis of Autism" section, we evaluate this model on a multisite study of autism. "Toward Characterizing Patient Heterogeneity" section presents a new extension of our framework that incorporates patient heterogeneity. Finally, we conclude with some general recommendations for future work in the field.

FUNCTIONAL CONNECTOMICS AS A WINDOW INTO ASD

Functional connectomics provides a unique glimpse into the steady-state organization of the brain. It is based on the underlying assumption that two regions, which reliably coactivate, are more likely to participate in similar neural processes than two uncorrelated or anticorrelated regions (Buckner and Vincent, 2007; Fox and Raichle, 2007; Van Dijk et al., 2010; Venkataraman et al., 2009). Over the past decade, functional connectomics has become ubiquitous in the study of neurological disorders, such as schizophrenia, epilepsy, and autism (DiMartino et al., 2014; Liang et al., 2006; Stufflebeam et al., 2011). From a practical standpoint, these functional relationships are often evaluated in resting-state fMRI (rsfMRI), which does not require patients to complete potentially challenging experimental paradigms. From a neuroscientific standpoint, group-level changes in the functional architecture of the brain may shed light on the etiological mechanisms of a disorder.

Univariate tests have historically been the standard approach to isolate the altered functional connectivity patterns in ASD (Cherkassky et al., 2006; Kennedy and Courchesne, 2008b). These methods identify statistical differences in pairwise similarity measures, such as Pearson correlation coefficients or seed-based correlation maps, as representative biomarkers of ASD. Perhaps the most notable findings have been a consistent reduction in interregional connections, particularly between the frontal and posterior lobes (Hull et al., 2016; Just et al., 2004, 2012), and connectivity differences linked to the default mode network (DMN), which activates during self-reflective processes (Buckner et al., 2008; Kennedy and Courchesne, 2008a; Padmanabhana et al., 2017). Interestingly, many studies have reported greater intraregional connectivity in some ASD subpopulations (Delmonte et al., 2013; DiMartino et al., 2014), which may be linked to enhanced sensory perception. Unfortunately, univariate results are wildly inconsistent across the ASD literature. One contributing factor to their low test-retest reliability is that, by construction, univariate tests ignore crucial dependencies across the brain (Venkataraman et al., 2010).

Graph models assume a structured relationship between the pairwise connectivity values to estimate surrogates of both functional specialization and functional integration (Achard and Bullmore, 2007; Bassett and Bullmore, 2009; Bullmore and Sporns, 2009; Rubinov and Sporns, 2010). For example, modularity and clustering coefficient quantify the interconnectedness of local processing units (functional specialization) (Meunier et al., 2009; Rubinov and Sporns, 2010; Sporns and Betzel, 2016), whereas average path length, global efficiency, and betweenness centrality quantify the reachability of each node in the network (functional integration) (Achard and Bullmore, 2007; Estrada and Hatano, 2008). Finally, the small-world architecture balances these competing influences (Tononi et al., 1994). The past 5 years has witnessed a proliferation in graph-theoretic studies of ASD. One interesting finding is a decrease in clustering coefficient and "hubness" across the brain, which suggests that, on average, ASD patients have a more random network organization than neurotypical controls (Itahashi et al., 2014). There has also been conflicting evidence to support the popular theory of local overconnectivity and long-range underconnectivity in ASD

(Takashi Itahashi et al., 2015; Keown et al., 2013; Redcay et al., 2013; Rudie and Dapretto, 2017). Although graph measures have provided some insight into ASD, they are markedly removed from the original network. Therefore, it is unclear what neural mechanisms contribute to these measures, whether group differences reflect a verifiable change in the underlying functional organization, or whether they stem from a confounding influence (Smith, 2012).

An alternate network approach is to decompose the rsfMRI time series into a collection of hidden sources in the brain. The increasingly popular independent component analysis (ICA) relies on statistical independence and non-Gaussianity to guide the network decomposition (Bell and Sejnowski, 1995; Calhoun et al., 2003; McKeown et al., 1998). When applied to rsfMRI data, ICA returns both a spatial map and a representative time series for each component/source (Calhoun et al., 2003, 2009). The anatomical organization of these components can be used to delineate different functional networks in the brain, and temporal fluctuations in the time series quantify the synchrony across networks. To a large extent, ICA studies for ASD focus on the similarity between selected ICA components (i.e., networks), such as the DMN (Assaf et al., 2010; Starck et al., 2013; Supekar et al., 2010), subcortical areas (Cerliani et al., 2015), the sensorimotor network (Nebel et al., 2014, 2016), and the prefrontal cortex (Starck et al., 2013). However, the main drawback of ICA is that it does not naturally generalize to multisubject or population level analyses (Calhoun et al., 2009).

Despite the breadth of analysis techniques, the previously discussed methods follow a similar two-step procedure for studying ASD: they first fit a connection- or graph-based model to the rsfMRI data and then identify group differences post hoc. In practice, this strategy tends to implicate distributed, and potentially unrelated, changes in functional connectivity across the brain. These isolated effects are difficult to interpret and are often missing crucial details about the functional architecture of the brain. To this end, we have developed a novel probabilistic framework that identifies *network-based differences* in functional connectivity. Our unique methodology extracts robust and clinically meaningful biomarkers of ASD from multisite connectivity data (Venkataraman et al., 2015). We also discuss a recently proposed extension of our model that incorporates a patient-specific measure of ASD severity into the Bayesian framework (Venkataraman et al., 2017).

AN UNBIASED BAYESIAN FRAMEWORK FOR FUNCTIONAL CONNECTOMICS

Given the growing perception of ASD as a system-level dysfunction (Courchesne and Pierce, 2005; Geschwind and Levitt, 2007), we hypothesize that the functional differences attributed to ASD reflect a set of *coordinated disruptions* in the brain. Although we do not specify a priori whether these disruptions occur within the same cognitive domain or whether they span multiple cognitive processes, we assume that the affected brain regions will communicate differently with other parts of the brain than if the disorder were not present. In the functional connectomics realm,

this underlying assumption can be modeled by region hubs, which exhibit a large number of altered functional connections, compared with the neurotypical cohort. In the following, we refer to these region hubs as *disease foci* and the altered functional connectivity patterns as *canonical networks.*

Fig. 1 outlines the generative process. The connectivity differences in ASD are explained by a set of K nonoverlapping networks, where K is a user-specified parameter that controls the model complexity. We use a probabilistic framework to represent the interaction between regions that describe the effects of ASD. Here, *latent* variables specify a template organization of the brain, which we cannot directly access. Instead, we observe noisy measurements of the hidden structure via rsfMRI correlations.

As seen, our framework is based on hierarchical variable interactions. The multinomial variable R_i indicates whether region i is healthy ($R_i = 0$) or whether it is a disease focus in network k ($R_i = k$). The latent functional connectivity F_{ij} describes the group-wise coactivation between region i and region j in the neurotypical controls based on one of three states: positive synchrony ($F_{ij} = 1$), negative synchrony ($F_{ij} = -1$), and no coactivation ($F_{ij} = 0$). Notice that our discrete representation of latent functional connectivity is a notable departure from conventional analysis. Specifically, we assume that rsfMRI correlations fall into one of three general categories, and differences in bin assignment are the relevant markers of ASD. Our choice of three states is motivated by the rsfMRI literature. For example, most works specify a threshold to determine functionally connected areas, which corresponds to $F_{ij} = 1$ in our framework. On the other hand, although strong negative correlations do appear in rsfMRI data, there is no consensus about their origin and significance (Van Dijk et al., 2010). Therefore, we isolate negative connectivity (i.e., $F_{ij} = -1$) as a separate category. The latent functional connectivity $\bar{F}_{ij}$ of the ASD population is also tristate and is defined via four simple rules: (1) a connection between two disease foci in the same network k is always abnormal, (2) a connection between two foci in different networks is never abnormal, (3) a connection between two healthy regions is never abnormal, and (4) a connection between a healthy and a diseased region is abnormal with probability η. Ideally $\bar{F}_{ij} \neq F_{ij}$ for abnormal connections and $\bar{F}_{ij} = F_{ij}$ for healthy connections. However, due to noise, we assume that the latent templates can deviate from these rules with probability ε. Notice that condition 2 ensures that the K networks remain distinct, and conditions 3 and 4 impose an outward spreading topology on the altered pathways. Finally, the rsfMRI correlations B_{ij}^{l} for neurotypical subject l and $\bar{B}_{ij}^{m}$ for ASD patient m are sampled from Gaussian distributions whose mean and variance depend on the neurotypical and ASD functional templates, respectively. The beauty of our proposed hierarchical model is that we are able to isolate the effects of ASD within the latent structure, while simultaneously accounting for noise and subject variability via the data likelihood.

We derive a variational expectation-maximization (EM) algorithm (Jordan et al., 1999) to estimate both the latent posterior probability of each region label q_i and the nonrandom model parameters from the observed data. A full mathematical characterization of the model and optimization algorithm are given in our previous publications (Venkataraman et al., 2015, 2013a).

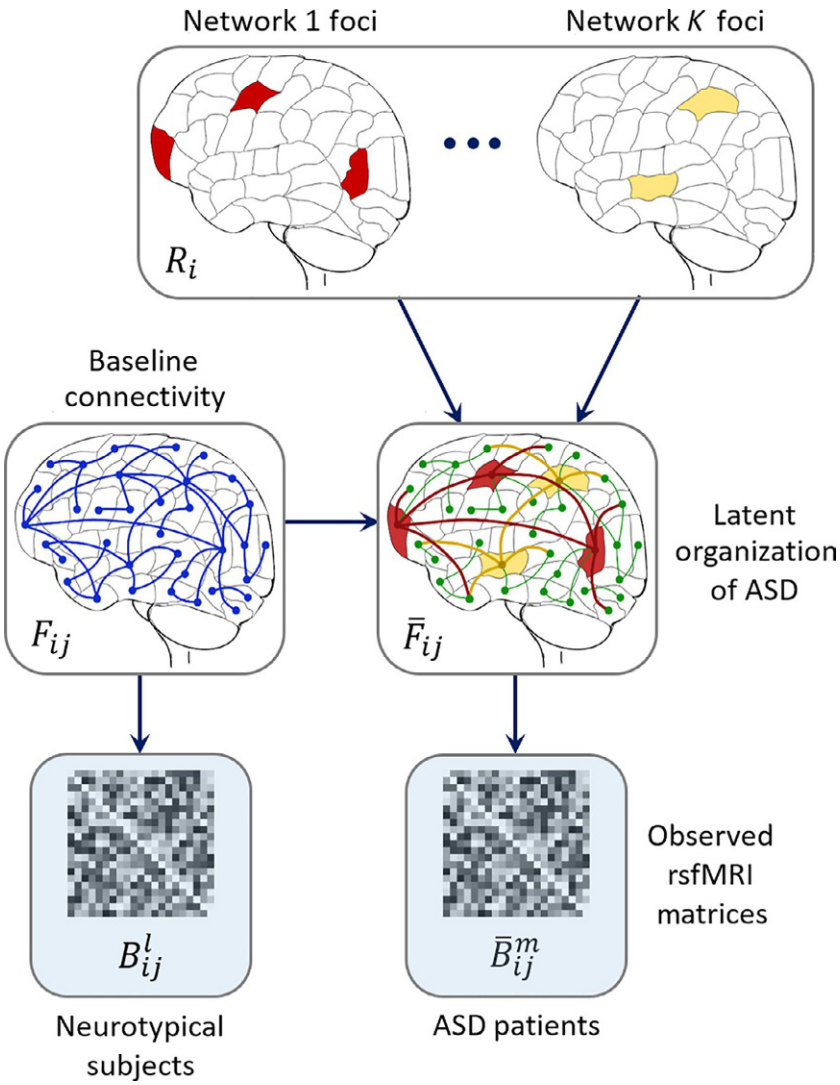

FIG. 1

Generative model of functional connectivity for ASD. Parcels correspond to regions in the brain, and lines denote pairwise functional connections. The label *Ri* indicates whether region *i* is healthy *(white)* or a focus in one of the *K* abnormal networks *(colored)*. These foci capture the most salient functional differences between patients and controls. The neurotypical template *Fij* provides a baseline functional architecture of the brain, whereas the clinical template $\bar{F}_{ij}$ specifies the functional differences attributed to ASD. The subject rsfMRI correlations $\{B^l_{ij}$ and $\{\bar{B}^m_{ij}\}$ are noisy observations of the latent functional templates.

Our methodology circumvents the interpretability challenges of the simple statistical analyses that currently dominate the clinical neuroscience literature. For example, univariate tests are commonly used to identify group-wise differences in pairwise correlation values. However, the bulk of our knowledge about the brain is organized around regions and not the connections between them. Moreover, connection-based results are nearly impossible to verify through direct stimulation. On the flipside, popular graph measures, such as modularity and small-worldness (Bassett and Bullmore, 2006; Honey et al., 2009; Rubinov and Sporns, 2010) collapse the rich network structures onto scalar values. As a result, we cannot tie statistical differences to a concrete etiological mechanism. In contrast, we explicitly model the propagation of information from regions (disease foci) to connections (canonical networks). Both of these variables have a straightforward biological meaning and can be used to design follow-up studies.

MULTISITE NETWORK ANALYSIS OF AUTISM

Our primary exploration of ASD relies on the publicly available and multisite autism brain imaging data exchange (ABIDE) (DiMartino et al., 2014). Given the variability of MR acquisition protocols across sites, we focus on four participating institutions, rather than filtering all subjects by some demographic criterion. These sites are the Yale Child Study Center, the Kennedy Krieger Institute, the University of California Los Angeles (Sample 1), and the University of Michigan (Sample 1).

EXPERIMENTAL SETUP

Subject selection: Our study focuses on children and adolescents, 7 to 19 years of age. Inclusion criteria for subjects within the chosen sites were based on both the acquisition quality and successful data preprocessing. On the acquisition front, we required whole-brain coverage and manual inspection of the MPRAGE and BOLD data quality. In addition, we excluded subjects who exhibited significant head motion (>0.5 mm translation or >0.5° rotation) in 25% or more time points of the BOLD series. On the preprocessing side, we verified accurate coregistration between the structural MPRAGE and functional BOLD images. We also filtered individuals for whom the distribution of region-wise rsfMRI correlations was markedly different from all other subjects, as measured by the Hellinger distance. In total, 260 subjects (141 neurotypical, 119 ASD) were selected for analysis. Additional details about the MR acquisition protocols and subject demographics can be found in Di Martino et al. (2014), and Venkataraman et al. (2015).

Data preprocessing: Our Bayesian framework in "An Unbiased Bayesian Framework for Functional Connectomics" section is based on region-wise connectivity measures. Region selection remains an open problem in functional connectomics.

For example, smaller regions are more susceptible to noise artifacts, whereas larger regions can potentially blur the relevant functional effects. This work relies on the Desikan-Killany atlas native to Freesurfer (Fischl et al., 2004), which segments the brain into 86 cortical and subcortical regions that roughly correspond to Broadman areas. The Desikan-Killany atlas provides anatomically meaningful correspondences across subjects that relate to functional divisions in the brain. We emphasize that our method can be applied to any set of consistently defined ROIs across subjects (e.g., the Supplementary Results of (Venkataraman et al., 2015)). The structural ROIs were then projected onto the subject-native fMRI space for each individual.

The BOLD rsfMRI data were processed using Functional MRI of the Brain's Software Library (FSL) (Smith et al., 2004) and in-house matrix laboratory (MATLAB) scripts (MATLAB, 2013). We discarded the first seven rsfMRI time points, and performed motion correction via rigid body alignment and slice timing correction using trilinear/sinc interpolation. The data were spatially smoothed using a Gaussian kernel with 5-mm full width at half maximum (FWHM) and band-pass filtered with cutoffs 0.01 and 0.1 Hz. Next, we regressed global contributions to the time courses from the white matter, ventricles, and whole brain to diminish the influence of physiological noise. Finally, we performed data scrubbing to remove consecutive time points with >0.5 mm translation or $>0.5^{\circ}$ rotation between them. We computed the observed rsfMRI connectivity measures as the Pearson correlation coefficient between the mean time courses within the two regions. These pairwise connectivity values were then aggregated into an 86×86 rsfMRI data matrix for each subject.

Evaluation criteria: We employed a rigorous evaluation strategy that included both quantitative measures of reproducibility and a qualitative assessment based on the fMRI literature.

Quantitatively, we evaluated the robustness of our approach in two ways: (1) nonparametric permutation tests for statistical significance and (2) bootstrapping experiments to confirm test-retest reliability. The permutation tests allowed us to estimate the null distribution of disease foci. Our procedure was to randomly assign the subject diagnoses (e.g., neurotypical vs ASD) 1000 times, fit the Bayesian model, and compute the region posterior probabilities q_i for each trial. The significance of region i is the proportion of permutations that yield a larger value of q_i for any of the K networks than is obtained under the true labeling. Notice that this is a particularly stringent criterion for $K > 1$, because the previous P-value does not account for interdependencies between the networks. In contrast, the bootstrapping experiment involves fitting the model using a subset of the data while preserving the ratio of neurotypical subjects to ASD patients. We intentionally did not control for other demographic or clinical variables (site, age, IQ, ADOS/ADI scores) to push the limits of our method on heterogeneous data. We resampled the random subsets multiple times and considered the average region posterior probability $\overline{q}_i$ across runs.

On the qualitative side, we leveraged the Neurosynth database (http://www.neurosynth.org/) to provide an unbiased and comprehensive evaluation of the functionality supported by each canonical network. Neurosynth aggregates both the activation

coordinates reported in prior fMRI studies and a set of descriptive words/phrases pulled from the abstracts. The metaanalytic framework uses the power of large datasets to calculate the posterior probability $P(Feature|Activation\ Coordinate)$ for a given psychological feature (i.e., word or phrase) at a particular spatial location (Yarkoni et al., 2011). In this way, we can identify constructs that have consistently been associated with a particular activation coordinate across a wide variety of fMRI studies and subject cohorts. At the time of our analysis, Neurosynth had precomputed and stored 3099 brain maps based on the previously discussed posterior information; each map is associated with a particular linguistic feature. Additionally, the website creators have used Latent Dirichlet Allocation (LDA) (Chang et al., 2013) to generate a set of high-level topics from the original 3099 words and phrases.

NETWORK-BASED DIFFERENCES IN ASD

From "An Unbiased Bayesian Framework for Functional Connectomics" section, we observe that the single free parameter of our model is the number of canonical networks K. This parameter can be set based on prior clinical knowledge, or we can sweep its value to track the evolution of canonical network foci with varying model complexity. This book chapter focuses on our result for $K = 2$ networks, which reveals a decoupling between social and language dysfunction in ASD. We refer the reader to our original publication (Venkataraman et al., 2015) and Supplementary Results for a more detailed exposition.

Canonical networks: Fig. 2 (left) illustrates the detected foci (region posterior probability $q_i > 0.5$) for $K = 2$ canonical networks. We have colored each region according to the uncorrected $-\log(P - value)$, such that red indicates low significance and yellow corresponds to high significance. Given the region foci, we can estimate the abnormal functional pathways based on the posterior differences between the neurotypical and ASD functional templates. These connections are shown in Fig. 2 (right) using the BrainNet Viewer toolbox for MATLAB (Xia et al., 2013).

Our primary network consists of four disease foci: the left middle temporal gyrus ($q_i = 0.97$, $P < .001$), the left posterior cingulate ($q_i = 1.00$, $P < .01$), the left supramarginal gyrus ($q_i = 1.00$, $P < .01$), and the right temporal pole ($q_i = 1.00$, $P < .05$). Interestingly, the abnormal pathways indicate a general reduction in long-range connectivity (blue lines) and an overall increase in short-range connectivity (magenta lines) in ASD. Our second network has lower significance and consists of the left banks of the middle superior temporal sulcus ($q_i = 1.00$, $P < .04$), the right posterior superior temporal sulcus extending into inferior parietal lobule ($q_i = 0.86$, $P < .08$), and the right middle temporal gyrus ($q_i = 0.98$, $P < .07$). We accepted a lower significance threshold for this network due to our stringent criteria of computing p-values for $K > 1$. The corresponding functional pathways demonstrate reduced interhemispheric connectivity but largely increased intrahemispheric connectivity.

Model robustness: Fig. 3 reports the average posterior probability in our test-retest experiments. We use half of the subjects in each trial while preserving the ratio of ASD patients to neurotypical controls. We have displayed only the regions for

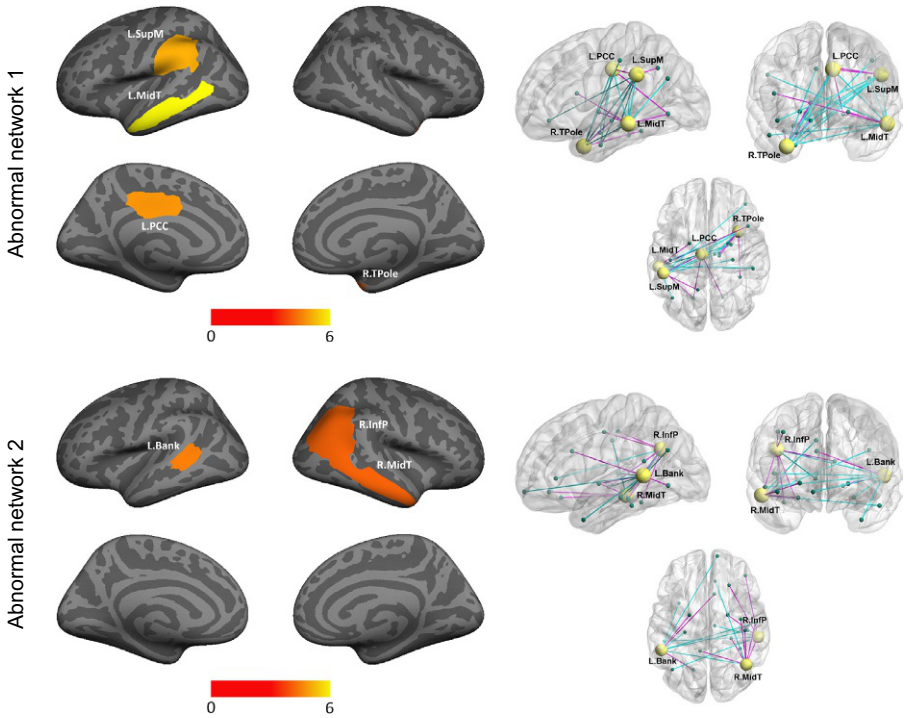

FIG. 2

Canonical networks inferred by our Bayesian model for $K = 2$ using the ABIDE dataset. Left: Significant regions based on permutation tests (region posterior probability $qi > 0.5$, uncorrected $P < .08$). Significance is computed via the likelihood of a region appearing in *either* network. The *color bar* corresponds to the negative log *P*-value. Right: Estimated graphs of abnormal functional connectivity in ASD. The *yellow nodes* correspond to disease foci. *Blue lines* indicated reduced functional connectivity in ASD, and *magenta lines* denote increased functional connectivity in ASD.

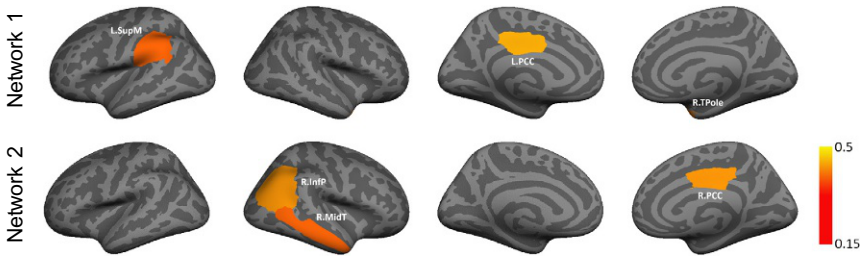

FIG. 3

Average marginal posterior probability *qi* for each network across 50 random samplings from the ABIDE dataset. Each subset includes 50% of the subjects, such that the ratio of ASD patients to neurotypical controls is preserved. The *color bar* denotes the average posterior probability. The highlighted regions correspond to the supramarginal gyrus (L.SupM), the inferior parietal cortex (R.InfP), the middle temporal gyrus (R.MidT), and the posterior cingulate (L.PCC and R.PCC).

which the average posterior probability across 50 random trials is >0.15—thereby emphasizing only the most prominent patterns. The color bar indicates the average probability, such that yellow denotes the strongest foci and red corresponds to the weakest influence. Remarkably, despite using only half of the data, our test-retest experiments are able to recover many of the disease foci from Fig. 2. This result verifies the generalizability of our framework for localizing robust functional connectivity differences in ASD.

Metaanalysis of the fMRI Literature: Fig. 4 illustrates our Neurosynth results. The upper panel describes the top 10 LDA topics implied by each set of network foci. We omitted topics that describe brain anatomy (e.g., default mode) or a neurological disorder (e.g., autism, which was among the top 10 for both networks). These mental states reveal both overlap and clear functional distinctions between the two intrinsic networks. Network 1 was associated with language-related topics, including comprehension and semantic processing. Network 2 also loaded heavily on language constructs but was uniquely associated with social-related topics, such as person and self-referential processing. The bottom panels of Fig. 4 display the relative correlation strengths of each topic generated by the Neurosynth decoder.

Implications for ASD: Language and communication deficits are among the defining features of ASD, as supported by our highly significant canonical network 1. Task-based fMRI has shed light on the system-level organization of language processing. For example, the upper band of the STS responds preferentially to the human voice, in comparison to other acoustic signals (Boddaert et al., 2003; Hickok, 2009). Going one step further, perception of meaningful speech localizes to the middle and inferior temporal cortices, whereas sentence comprehension tasks activate the bilateral superior temporal gyri (Price, 2009). On the other hand, canonical network 2 pinpoints a well-known social perception pathway centered in the right posterior STS, extending into the inferior parietal lobule and right middle temporal gyrus (Yang et al., 2015). The posterior STS is sensitive to and selective for social stimuli that signal intent in humans (Jastorff et al., 2012). In the visual domain, it activates preferentially to faces versus objects and to socially meaningful human actions versus nongoal-directed movements (Bahnemann et al., 2010; Gobbini and Haxby, 2007; Watson et al., 2014). In the auditory domain, the posterior STS responds to auditory speech (Ethofer et al., 2006; Wildgruber et al., 2006). Finally, the posterior STS is functionally interconnected to all the key regions of the "social brain" (Yang et al., 2015).

In addition to the region foci, the altered functional pathways are highly relevant to current theories of ASD. Specifically, our canonical networks support a general reduction in long-range connectivity, both within and across the hemispheres. These long-range connections likely correspond to integration processes, which are essential to higher order social, emotional, and communicative functioning (Oberman and Ramachandran, 2008; Rippon et al., 2007; Wolff et al., 2012). It is believed that disruptions in long-range connectivity play a key role in the hallmark dysfunctions of ASD. Likewise, hemispheric abnormalities are prevalent in the ASD literature, particularly within the language domain (Dawson et al., 1989; Redcay and Courchesne, 2008).

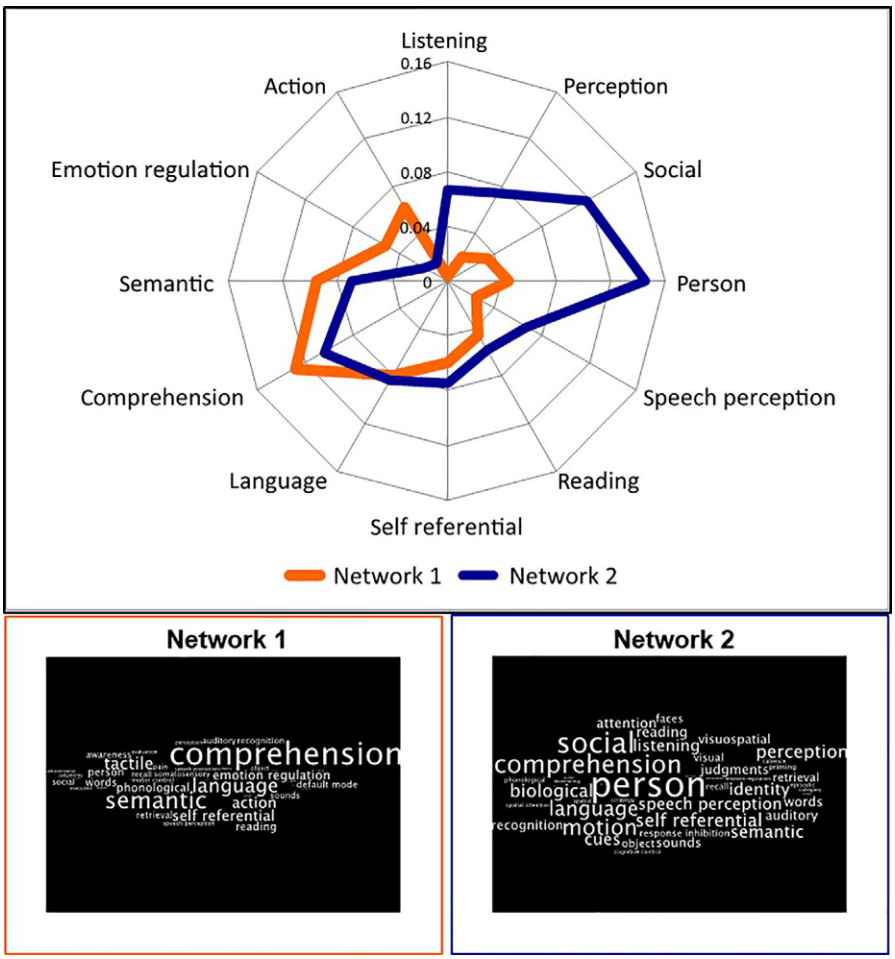

FIG. 4

Upper: correlation values of the top 10 topics for each network, which represent the specificity of neurocognitive functions derived from metaanalytic decoding. We include words that overlap between networks, resulting in 14 total features. Lower: relative rankings of the psychological constructs. Word size reflects rank-ordered correlation coefficients, which emphasizes terms most associated with each network (Poldrack et al., 2009).

In contrast, both canonical networks also find a general increase in short-range connectivity, which may contribute to enhanced cognitive and pattern recognition skills often reported in high-functioning ASD subpopulations (Johnson et al., 2002).

It is worth mentioning that our framework does not implicate certain regions that have been previously reported in the ASD literature. Examples include the prefrontal cortex, as related to working memory and executive function (Baron-Cohen et al., 1999;

Courchesne and Pierce, 2005; Gilbert et al., 2008; Just et al., 2004), and the visuomotor cortex (Dowell et al., 2009; Koshino et al., 2008; Mostofsky and Ewen, 2011; Nebel et al., 2016). One possibility is that such differences are overwhelmed by the intersite variability, including scanner model, acquisition procedures, and subject recruitment. Another possibility is that there is weak evidence in our cohort to support the prefrontal and visuomotor cortices acting as foci. Recall that our model is completely data-driven and does not impose spatial constraints on the canonical networks. Finally, it is possible that our region parcellation is too coarse to identify these additional effects.

We conclude this section by addressing the model complexity parameter K, which specifies the number of canonical networks that explain the data. Intuitively, there will be a tradeoff between model robustness and our ability to pinpoint weaker effects. Due to the lack of ground-truth connectivity information, we have constructed both quantitative and qualitative proxies for generalizability and relevance, which can be used to evaluate the impact of K. Taken together, the results in this chapter demonstrate the power of our hierarchical Bayesian framework as a future analysis tool for ASD.

TOWARD CHARACTERIZING PATIENT HETEROGENEITY

As described earlier in this chapter, ASD is a notoriously heterogeneous disorder that includes both a wide variety of behavioral symptoms and a range of clinical severity. As previously alluded to, the existing ASD literature implicitly treats the patient group as homogenous, for example, by conducting a statistical evaluation that separates patients from controls. Even our unbiased Bayesian framework infers a single functional template for the entire ASD cohort. It has been argued that this gross simplification is partially responsible for the lack of reproducible fMRI findings in much of the clinical neuroscience literature (Horga et al., 2014).

This section tackles a fundamental yet commonly overlooked question in the study of functional connectomics: how do we identify the altered functional pathways given a heterogeneous patient cohort? As a first step, we consider a one-dimensional measure of clinical severity and a single canonical network ($K = 1$). We fold the behavioral information into our probabilistic framework by stipulating that the canonical network influence on an individual patient is moderated by their scalar severity score. Said another way, patients with higher ASD severity scores will manifest *more* network dysfunction than patients with lower ASD severity. Hence, rather than dismissing or regressing out the clinical scores, these measures will crucially guide our network estimation procedures.

Fig. 5 illustrates the revised interactions. As seen, the strengths of the canonical network edges are proportional to behavioral score $\beta_m \in [0, 1]$, which can be quantified via neuropsychiatric testing or parent questionnaires. Effectively, the patient likelihood weighs the relative contributions of the clinical and neurotypical templates via β_m. Mathematically, the patient rsfMRI correlation $\bar{B}_{ij}^m$ is sampled from

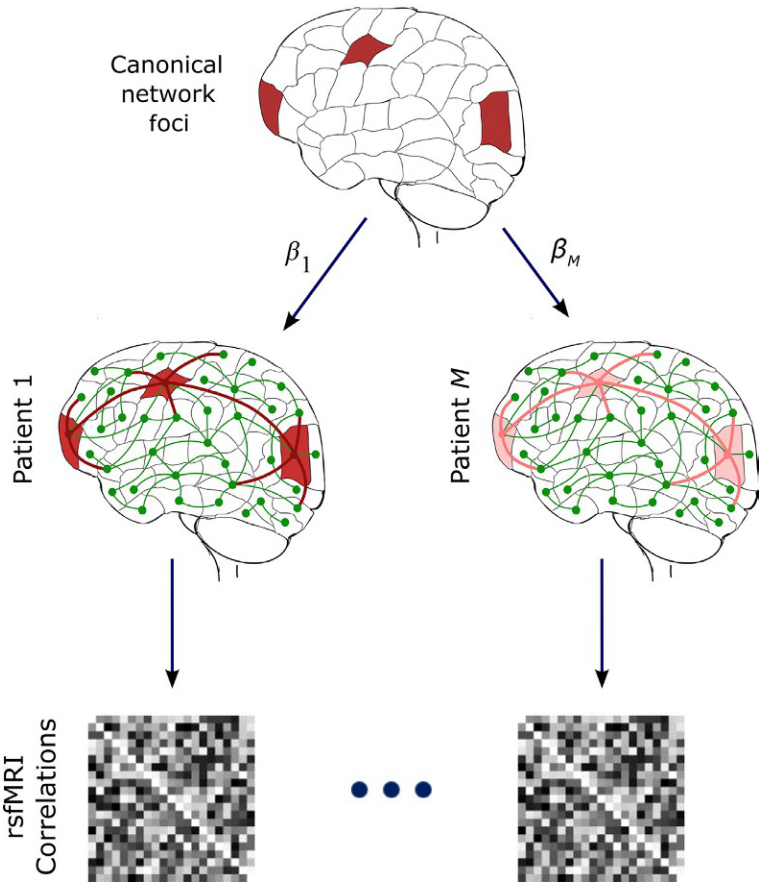

FIG. 5

Conceptual diagram of behavioral influence. *Red regions* correspond to the disease foci, and *red edges* specify the canonical functional network. *Green edges* are normal (i.e., healthy) connections. The canonical network contribution for each patient m is specified by the clinical severity, $\beta m \in [0, 1]$. Here, $\beta_1 > \beta M$, as indicated by the *darker edges*.

the Gaussian distribution specified by the ASD template with probability β_m, and it is sampled from the Gaussian distribution associated with the neurotypical template with probability $1 - \beta_m$.

EXPERIMENTAL SETUP

Study participants: To avoid site artifacts, we rely on a much tighter sample drawn from the Kennedy Krieger Institute in Baltimore, MD. Our dataset consists of 66 high-functioning, school-aged children with ASD and 66 neurotypical controls, who

were matched on the basis of age, gender, and IQ. The severity measures β_m in our analysis correspond to the Autism Diagnostic Observation Schedule (ADOS) total raw score (Gotham et al., 2007), normalized by the maximum possible test score.

Data preprocessing: Once again, we must define consistent region boundaries for our model. In this section, we rely on the Automatic Anatomical Labeling (AAL) atlas (Tzourio-Mazoyer et al., 2002) to delineate 116 cortical, subcortical, and cerebellar regions. RsfMRI preprocessing was implemented using the Statistical Parametric Mapping (SPM) toolbox, in-house MATLAB scripts, and the Analysis of Functional NeuroImages (AFNI) package (Cox, 1996). Our basic fMRI pipeline included slice timing correction, rigid body realignment, and normalization to the EPI version of the MNI template. To facilitate the connectivity analyses, we temporally detrended the time series and used CompCorr to estimate and remove spatially coherent noise from the white matter, ventricles, motion parameters, and their first derivatives (Behzadi et al., 2007). The cleaned data was spatially smoothed with a 6-mm FWHM Gaussian kernel, temporally filtered and spike-corrected. Similar to the previous section, our rsfMRI measures are computed as the Pearson correlation coefficients between the mean time courses in the two regions. We focus on deviations from baseline synchrony by centering the whole-brain correlation histograms for each subject.

Evaluation criteria: Similar to the previous section, we evaluated the test-retest reliability of our region assignments q_i via bootstrapping. Specifically, we fitted the heterogeneous model to random subsets of the data while preserving the ratio of ASD patients to neurotypical controls. We ran two analyses, which corresponded to subsets with 90% and 50% of the overall cohort. Our quantitative measure of robustness is the average region posterior probability across 100 random trials. In addition to bootstrapping, we performed a qualitative comparison of this revised Bayesian model with our original framework in "An Unbiased Bayesian Framework for Functional Connectomics" section and with univariate *t*-tests on the pairwise rsfMRI correlation values.

NETWORK DYSFUNCTION LINKED TO ASD SEVERITY

Heterogeneous network architecture: Fig. 6 illustrates the single canonical network inferred by our model. The yellow nodes correspond to the disease foci, and we have displayed connections consistently implicated across bootstrapping trials. Similar to the previous section, the magenta and blue lines denote increased and reduced latent connectivity in ASD relative to the neurotypical population. As seen, our model identifies four disease foci: the right precentral gyrus (R.PreCG), the right posterior cingulate gyrus (R.PCG), the right angular gyrus (R.ANG), and vermis 8 of the cerebellum (Verm8).

Our results are closely aligned with recent findings in ASD. For example, the right precentral gyrus and cerebellar vermis represent foci specialized in the production of actions, a core behavioral feature consistently reported in ASD

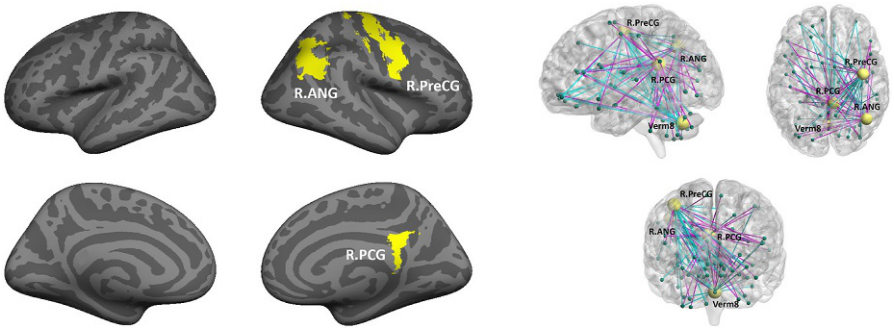

FIG. 6

Results of our heterogeneous patient model. Left: disease foci projected onto the inflated cortical surface. Right: canonical network of abnormal functional connectivity. *Yellow nodes* correspond to the disease foci. *Blue lines* signify reduced functional connectivity in ASD; *magenta lines* denote increased functional connectivity in ASD.

(Mostofsky and Ewen, 2011; Nebel et al., 2016). Moreover, the right angular gyrus and posterior cingulate are common to the DMN, which is believed to moderate internal reflective processes (Buckner et al., 2008). Converging multimodal evidence suggests that the altered functional and structural organization of the DMN contributes to social cognitive dysfunction in ASD (Padmanabhana et al., 2017). In this manner, our canonical network seems to represent the consequence of abnormal development and compensatory mechanisms for the expression of social and communicative functions.

Model robustness: Fig. 7 reports the average posterior probability $\overline{q}_i$ of each region across 100 bootstrapped trials. We display only the regions for which $\overline{q}_i > 0.3$ to emphasize the most prominent patterns. Notice that our model consistently recovers

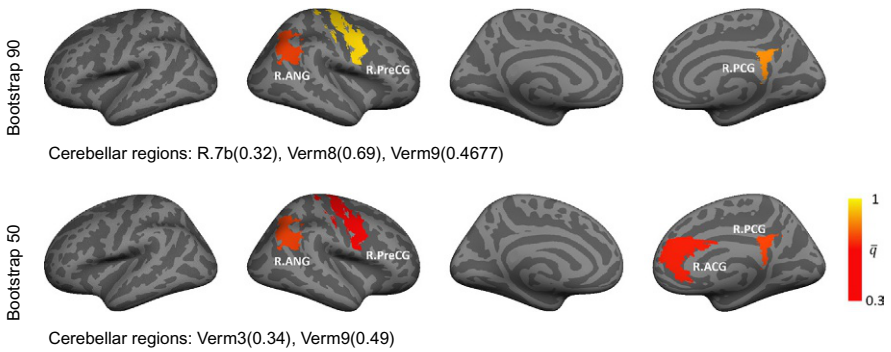

FIG. 7

Average marginal posterior probability $\overline{q}_i$ for each community across 100 random samplings of the rsfMRI dataset. Top row includes 90% of the subjects in each subset, and the bottom row includes 50%. Reproducibility of cerebellar regions are listed underneath.

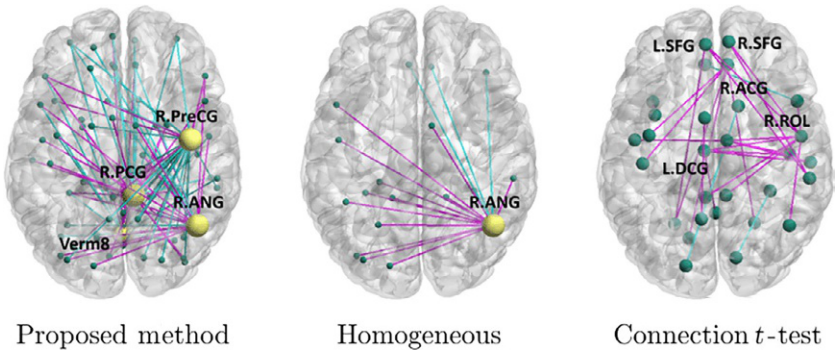

FIG. 8

Qualitative comparison of our heterogeneous patient model (left), the original Bayesian model described in "An Unbiased Bayesian Framework for Functional Connectomics" section, and the top connections ($P < .001$ uncorrected) identified via two-sample t-tests on the pairwise correlation values (right).

the canonical network foci in Fig. 6 when trained on 90% of the data. Remarkably, we are still able to detect the original network foci using just half the dataset, which further validates the reproducibility of our revised Bayesian framework. In fact, we note that the robustness in Fig. 7 is markedly higher than in our initial ABIDE study, in part due to stricter control over the subject recruitment and MR acquisition protocols. Finally, our bootstrapping experiments also implicate cerebellar regions adjacent to Vermis 8, which ties into broader theories of altered cerebellar functioning in ASD (Becker and Stoodley, 2013).

Baseline comparisons: Fig. 8 compares our heterogeneous canonical network (left) with our original Bayesian model (middle), which assumes a homogeneous patient group, and with standard univariate tests (right). Notice that the homogeneous model identifies a single disease focus in the DMN (R.ANG). However, incorporating the severity scores β_m seems to provide an additional level of flexibility, which allows us to find more subtle effects in other brain regions. On the other hand, connections implicated by two-sample t-tests form a markedly different pattern than our network model results. First, the univariate tests implicate several isolated connections, which are difficult to interpret. Second, the connections tend to concentrate in the frontal cortex and anterior cingulate gyrus, rather than the DMN. This observation suggests that our disease foci are unveiling a unique facet of the rsfMRI data.

CONCLUDING REMARKS

Functional connectomics has become a universal tool to noninvasively assess neural interactions on a global scale. Going one step further, it allows us to isolate system-level dysfunctions induced by a complex neurological disorder, such as ASD. Recent findings have confirmed a general reduction in long-range connectivity

between functional systems, which may be linked to integrative processes, such as social awareness and emotional perception. Graph theoretic studies suggest that the autistic brain might be more "randomly" organized than a neurotypical brain. However, despite the wealth of research and publications, we have yet to identify robust rsfMRI biomarkers for the disorder. This paradox can be explained by one of two possibilities: either the null hypothesis is true and rsfMRI does not contain enough information to be clinically relevant for ASD, or we have not sufficiently explored the methods that can describe the functional abnormalities, while handling the quirks of rsfMRI data.

In an effort to address this conundrum, we have devoted the bulk of this chapter to a novel probabilistic framework that contributes two unexplored dimensions to current network analytics: (1) we assume that the *functional differences* attributed to ASD form their own subnetwork, and (2) we explicitly model clinical severity. The corresponding network architectures confirm theories of both impaired social communication and reduced sensorimotor integration in ASD. Our results are quantitatively verified via nonparametric permutation testing and test-retest reliability experiments. Equally exciting, our Bayesian model can be adapted to a variety of technical challenges from detecting abnormal patterns in task fMRI (Venkataraman et al., 2016a, b), evaluating pre- versus posttreatment connectivity differences (Venkataraman et al., 2016a, b), multimodal integration with diffusion MRI (Venkataraman et al., 2013b), and a patient-specific analysis (Sweet et al., 2013). On the clinical side, our framework has been applied to ASD, schizophrenia, posttraumatic stress disorder, mild traumatic brain injury, and epilepsy.

Looking forward, there are a number of challenges that we, as a field, must address with respect to the functional connectomics of ASD. One obvious factor is patient heterogeneity. "Toward Characterizing Patient Heterogeneity" section takes a first step of incorporating clinical severity into the network decomposition. However, ASD is characterized by a multitude of behavioral and cognitive symptoms, from impaired social skills to language problems to stereotyped behaviors. To complicate matters, full-scale intelligence also plays a role in functional connectivity. Future methods should leverage this variability to provide a more complete picture of the disorder. A second challenge is to develop methods that are robust to data acquisition and image quality, while providing interpretable information about ASD. The issue of interpretability will become increasingly relevant in the next few years given the rise of artificial intelligence. In particular, while neural networks and deep learning can achieve impressive detection and regression performance, they are essentially black-box functions, which provide little insight as to what patterns in the data are meaningful and why. Along the same lines, a third goal is to formalize new evaluation metrics. At present, statistical significance dominates the ASD literature, but p-values are often poor indicators of test-retest reliability (Venkataraman et al., 2010). Finally, we close this chapter on a philosophical note. Functional connectomics has been invaluable to studying and probing complex questions related to ASD. We have found, albeit contradictory, patterns related to higher level cognitive functions, such as social awareness and sensory integration. But what comes next? How do we translate these findings into a real-world impact at the patient level? These questions should fuel the next great wave of autism research.

REFERENCES

Achard, S., Bullmore, E., 2007. Efficiency and cost of economical brain functional networks. PLoS Comput. Biol. 3 (2), 1–10.

Americal Psychiatric Association, 2013. Diagnostic and Statistical Manual of Mental Disorders, fifth ed. American Psychiatric Publishing, Arlington, VA.

Aoki, Y., Abe, O., Nippashi, Y., Yamasue, H., 2013. Comparison of white matter integrity between autism spectrum disorder subjects and typically developing individuals: a meta-analysis of diffusion tensor imaging Tractography studies. Mol. Autism 4 (1), 25.

Assaf, M., Jagannathan, K., Calhoun, V.D., Miller, L., Stevens, M.C., Sahl, R., 2010. Abnormal functional connectivity of default mode sub-networks in autism spectrum disorder patients. Neuroimage 53, https://doi.org/10.1016/j.neuroimage.2010.05.067.

Bahnemann, M., Dziobek, I., Prehn, K., Wolf, I., Heekeren, H.R., 2010. Sociotopy in the temporoparietal cortex: common versus distinct processes. Soc. Cogn. Affect. Neurosci. 5 (1), 48–58. https://doi.org/10.1093/scan/nsp045.

Baron-Cohen, S., Ring, H.A., Wheelwright, S., Bullmore, E.T., Brammer, M.J., Simmons, A., Williams, S.C.R., 1999. Social intelligence in the normal and autistic brain: an fMRI study. Eur. J. Neurosci. 11 (6), 1891–1898. https://doi.org/10.1046/j.1460-9568.1999.00621.x.

Bassett, D.S., Bullmore, E., 2006. Small-world brain networks. Neuroscientist 12, 512–523.

Bassett, D.S., Bullmore, E., 2009. Human brain networks in health and disease. Curr. Opin. Neurol. 22, 340–347.

Becker, E., Stoodley, C., 2013. Autism spectrum disorder and the cerebellum. Int. Rev. Neurobiol. 113, 1–34.

Behzadi, Y., Restom, K., Liau, J., Liu, T.T., 2007. A component based noise correction method (CompCor) for BOLD and perfusion based fMRI. Neuroimage 37 (1), 90–101.

Bell, A.J., Sejnowski, T.J., 1995. An information-maximization approach to blind separation and blind deconvolution. Neural Comput. 7, 1129–1159.

Belmonte, M.K., Yurgelun-Todd, D.A., 2003. Functional anatomy of impaired selective attention and compensatory processing in autism. Cogn. Brain Res. 17 (3), 651–664. https://doi.org/10.1016/S0926-6410(03)00189-7.

Boddaert, N., Belin, P., Chabane, N., Poline, J.B., Barthélémy, C., Mouren-Simeoni, M.C., Zilbovicius, M., 2003. Perception of complex sounds: abnormal pattern of cortical activation in autism. Am. J. Psychiatry 160 (11), 2057–2060. Retrieved from, http://view.ncbi.nlm.nih.gov/pubmed/14594758.

Buckner, R.L., Vincent, J.L., 2007. Unrest at rest: default activity and spontaneous network correlations. Neuroimage 37 (4), 1091–1096.

Buckner, R.L., Andrews-Hanna, J.R., Schacter, D.L., 2008. The Brain's default network anatomy, function, and relevence to disease. Ann. NY Acad. Sci. 1124, 1–38.

Bullmore, E., Sporns, O., 2009. Complex brain networks: graph theoretical analysis of structural and functional systems. Nat. Rev. Neurosci. 10, 186–198.

Calhoun, V.D., Adali, T., Hansen, L.K., Larsen, J., Pekar, J.J., 2003. In: *ICA of Functional MRI Data: An Overview*. *The 4th International Symposium on Independent Component Analysis and Blind Signal Separation*, pp. 281–288.

Calhoun, V.D., Liu, J., Adalı, T., 2009. A review of group ICA for fMRI data and ICA for joint inference of imaging, genetic, and ERP data. Neuroimage 45, S163–S172.

Centers for for Disease Control, 2012. Prevalence of autism spectrum disorders—autism and developmental disabilities monitoring network, 14 sites, United States, 2008. MMWR 61 (3), 1–19.

Cerliani, L., Mennes, M., Thomas, R.M., Di Martino, A., Thioux, M., Keysers, C., 2015. Increased functional connectivity between subcortical and cortical resting-state networks in autism Spectrum disorder. JAMA Psychiat. 72 (8), 767–777. https://doi.org/10.1001/jamapsychiatry.2015.0101.

Chang, L.J., Yarkoni, T., Khaw, M.W., Sanfey, A.G., 2013. Decoding the role of the insula in human cognition: functional parcellation and large-scale reverse inference. Cereb. Cortex 23 (3), 739–749. https://doi.org/10.1093/cercor/bhs065.

Cherkassky, V.L., Kana, R.K., Keller, T.A., Just, M.A., 2006. Functional connectivity in a baseline resting-state network in autism. Neuroreport 17 (16), 1687–1690.

Courchesne, E., Pierce, K., 2005. Why the frontal cortex in autism might be talking only to itself: Local over-connectivity but long-distance disconnection. Curr. Opin. Neurobiol. 15, 225–230.

Cox, R.W., 1996. AFNI: software for analysis and visualization of functional magnetic resonance neuroimages. Comput. Biomed. Res. 29 (3), 162–173.

Dawson, G., Finley, C., Phillips, S., Lewy, A., 1989. A comparison of hemispheric asymmetries in speech related brain potentials of autistic and dysphasic children. Brain Lang. 37 (1), 26–41.

Delmonte, S., Gallagher, L., O'Hanlon, E., McGrath, J., Balsters, J.H., 2013. Functional and structural connectivity of frontostriatal circuitry in autism spectrum disorder. Front. Hum. Neurosci. 7, 430. https://doi.org/10.3389/fnhum.2013.00430.

Di Martino, A., Yan, C.-G., Li, Q., Denio, E., Castellanos, F.X., Alaerts, K., Milham, M.P., 2014. The autism brain imaging data exchange: towards a large-scale evaluation of the intrinsic brain architecture in autism. Mol. Psychiatry 19, 659–667.

DiMartino, A., Yan, C.G., Li, Q., Denio, E., Castellanos, F.X., Alaerts, K., et al., 2014. The autism brain imaging data exchange: towards a large-scale evaluation of the intrinsic brain architecture in autism. Mol. Psychiatry 19 (6), https://doi.org/10.1038/mp.2013.78.

Dowell, L.R., Mahone, M.E., Mostofsky, S.H., 2009. Associations of postural knowledge and basic motor skill with dyspraxia in autism: Implication for abnormalities in distributed connectivity and motor learning. Neuropsychology 23 (5), 563–570.

Estrada, E., Hatano, N., 2008. Communicability in complex networks. Phys. Rev. Stat. 77, 036111.

Ethofer, T., Anders, S., Erb, M., Herbert, C., Wiethoff, S., Kissler, J., Crodd, W., Wildgruber, D., 2006. Cerebral pathways in processing of affective prosody: a dynamic causal modeling study. Neuroimage 30 (2), 580–587. https://doi.org/10.1016/j.neuroimage.2005.09.059.

Fischl, B., Salat, D.H., van der Kouwe, A.J.W., Makris, N., Ségonne, F., Quinn, B.T., Dale, A.M., 2004. Sequence-independent segmentation of magnetic resonance images. Neuroimage 23, 69–84.

Fox, M.D., Raichle, M.E., 2007. Spontaneous fluctuations in brain activity observed with functional magnetic resonance imaging. Nature 8, 700–711.

Gabrieli-Whitfield, S., Thermenos, H.W., Milanovic, Z., Tsuang, M.T., Faraone, S.V., McCarley, R.W., Shenton, M.E., Green, A.I., Nieto-Castanon, A., La Violette, P., Wojcik, J., Gabrieli, J.D., Seidman, L.J., 2009. Hyperactivity and Hyperconnectivity of the default network in schizophrenia and in first-degree relatives of persons with schizophrenia. Natl. Acad. Sci. USA 106, 1279–1284.

Geschwind, D.H., Konopka, G., 2009. Neuroscience in the era of functional genomics and systems biology. Nature 461 (7266), 908–915.

Geschwind, D.H., Levitt, P., 2007. Autism spectrum disorders: developmental disconnection syndromes. Curr. Opin. Neurobiol. 17, 103–111.

Gilbert, S.J., Bird, G., Brindley, R., Frith, C.D., Burgess, P.W., 2008. A typical recruitment of medial prefrontal cortex in autism spectrum disorders: an fMRI study of two executive function tasks. Neuropsychologia 46 (9), 2281–2291. https://doi.org/10.1016/j.neuropsychologia.2008.03.025.

Globerson, E., Amir, N., Kishon-Rabin, L., Golan, O., 2015. Prosody recognition in adults with high-functioning autism Spectrum disorders: from psychoacoustics to cognition. Autism Res. 8 (2), 153–163.

Gobbini, M.I., Haxby, J.V., 2007. Neural systems for recognition of familiar faces. Neuropsychologia 45 (1), 32–41. Retrieved from, http://view.ncbi.nlm.nih.gov/pubmed/16797608.

Gotham, K., Risi, S., Pickles, A., Lord, C., 2007. The autism diagnostic observation schedule: revised algorithms for improved diagnostic validity. J. Autism Dev. Disord. 37, 613–627.

Grossman, R.B., Bemis, R.H., Plesa Skwerer, D., Tager-Flusberg, H., 2010. Lexical and affective prosody in children with high-functioning autism. J. Speech Lang. Hear. Res. 53 (3), 778–793.

Hernandez, L.M., Rudie, J.D., Green, S.A., Bookheimer, S., Dapretto, M., 2015. Neural signatures of autism spectrum disorders: insights into brain network dynamics. Neuropsychopharmacol. Rev. 40 (1), 171–189.

Hickok, G., 2009. The functional neuroanatomy of language. Phys. Life Rev. 6 (3), 121–143. https://doi.org/10.1016/j.plrev.2009.06.001.

Honey, C.J., Sporns, O., Cammoun, L., Gigandet, X., Thiran, J.P., Meuli, R., Hagmann, P., 2009. Predicting human resting-state functional connectivity from structural connectivity. Proc. Natl. Acad. Sci. 106, 2035–2040.

Horga, G., Kaur, T., Peterson, B.S., 2014. Annual research review: Current limitations and future directions in {MRI} studies of child- and adult-onset developmental psychopathologies. J. Child Psychol. Psychiatry 55 (6), 659–680.

Hull, J.V., Jacokes, Z.J., Torgerson, C.M., Irimia, A., Van Horn, J.D., 2016. Resting-state functional connectivity in autism Spectrum disorders: a review. Front. Psych. 7, 205. https://doi.org/10.3389/fpsyt.2016.00205.

Itahashi, T., Yamada, T., Watanabe, H., Nakamura, M., Jimbo, D., Shioda, S., Hashimoto, R., 2014. Altered network topologies and hub organization in adults with autism: a resting-state fMRI study. PLoS One 9 (4), e94115.

Itahashi, T., Yamada, T., Watanabe, H., Nakamura, M., Ohta, H., Kanai, C., Hashimoto, R., 2015. Alterations of local spontaneous brain activity and connectivity in adults with high-functioning autism Spectrum disorder. Mol. Autism 6 (1), 30. https://doi.org/10.1186/s13229-015-0026-z.

Jastorff, J., Popivanov, I.D., Vogels, R., Vanduffel, W., Orban, G.A., 2012. Integration of shape and motion cues in biological motion processing in the monkey STS. Neuroimage 60 (2), 911–921. https://doi.org/10.1016/j.neuroimage.2011.12.087.

Johnson, M.H., Halit, H., Grice, S.J., Karmiloff-Smith, A., 2002. Neuroimaging of typical and atypical development: a perspective from multiple levels of analysis. Dev. Psychopathol. 41, 521–536.

Jordan, M.I., Ghahramani, Z., Jaakkola, T.S., Saul, L.K., 1999. An introduction to variational methods for graphical models. Mach. Learn. 37, 183–233.

Just, M.A., Cherkassky, V.L., Keller, T.A., Minshew, N.J., 2004. Cortical activation and synchronization during sentence comprehension in high-functioning autism: evidence of underconnectivity. Brain 127, 1811–1821.

Just, M.A., Keller, T.A., Malavea, V.L., Kana, R.K., Varmac, S., 2012. Autism as a neural systems disorder: a theory of frontal-posterior underconnectivity. Neurosci. Biobehav. Rev. 36, 1292–1313.

Kanner, L., 1943. Autistic disturbances of affective contact. Neurodiver. Child. 2, 217–250.

Kennedy, D.P., Courchesne, E., 2008a. Functional abnormalities of the default network during self-and other-reflection in autism. Soc. Cogn. Affect. Neurosci. 3, 177–190.

Kennedy, D.P., Courchesne, E., 2008b. The intrinsic functional organization of the brain is altered in autism. Neuroimage 39, 1877–1887.

Keown, C.L., Shih, P., Nair, A., Peterson, N., Mulvey, M.E., Muller, R.A., 2013. Local functional overconnectivity in posterior brain regions is associated with symptom severity in autism spectrum disorders. Cell Rep. 5, 567–572.

Kleinhans, N.M., Müller, R.A., Cohen, D.N., Courchesne, E., 2008. Atypical functional lateralization of language in autism spectrum disorders. Brain Res. 1221, 115–125. https://doi.org/10.1016/j.brainres.2008.04.080.

Koshino, H., Carpenter, P.A., Minshew, N.J., Cherkassky, V.L., Keller, T.A., Just, M.A., 2005. Functional connectivity in an fMRI working memory task in high-functioning autism. Neuroimage 24 (3), 810–821.

Koshino, H., Kana, R.K., Keller, T.A., Cherkassky, V.L., Minshew, N.J., Just, M.A., 2008. fMRI investigation of working memory for faces in autism: visual coding and underconnectivity with frontal areas. Cereb. Cortex 18 (2), 289–300.

Leslie, D.L., Martin, A., 2007. Health care expenditures associated with autism spectrum disorders. Arch. Pediatr. Adolesc. Med. 161 (4), 350–355.

Liang, M., Zhou, Y., Jiang, T., Liu, Z., Tian, L., Liu, H., Hao, Y., 2006. Widespread functional disconnectivity in schizophrenia with resting-state functional magnetic resonance imaging. Neuro Rep Brain Imag 17 (2), 209–213.

MATLAB, 2013. Version 8.2.0.701 (R2013b). The MathWorks Inc, Natick, MA.

McKeown, M.J., Makeig, S., Brown, G.G., Jung, T.-P., Kindermann, S.S., Bell, A.J., Sejnowski, T.J., 1998. Analysis of fMRI data by blind separation into spatial independent components. Hum. Brain Mapp. 6, 160–188.

Melillo, R., Leisman, G., 2011. Autistic spectrum disorders as functional disconnection syndrome. Rev. Neurosci. 20 (2), 111–131.

Meunier, D., Lambiotte, R., Fornito, A., Ersche, K.D., Bullmore, E.T., 2009. Hierarchical modularity in human brain functional networks. Front. Neuroinform. 3, 37.

Mostofsky, S.H., Ewen, J.B., 2011. Altered connectivity and action model formation in autism. Neuroscientist 17, 437–448.

Nebel, M.B., et al., 2014. Precentral gyrus functional connectivity signatures of autism. Front. Syst. Neurosci. 8, 1–11.

Nebel, M.B., Eloyan, A., Nettles, C.A., Sweeney, K.L., Ament, K., Ward, R.E., Choe, A.S., Barber, A.D., Pekar, J.J., Mostofsky, S.H., 2016. Intrinsic visual-motor synchrony correlates with social deficits in autism. Biol. Psychiatry 79, 633–641.

Oberman, L.M., Ramachandran, V.S., 2008. Preliminary evidence for deficits in multisensory integration in autism spectrum disorders: The mirror neuron hypothesis. Soc. Neurosci. 3, 348–355.

Padmanabhana, A., Lynchd, C.J., Schaere, M., Menon, V., 2017. The default mode network in autism. Biol. Psych. Cogn. Neurosci. Neuroimag. 2 (6), 476–486.

Pelphrey, K.A., Yang, D.-J., McPartland, J.C., 2014. Building a social neuroscience of autism spectrum disorder. Curr. Top. Behav. Neurosci. 16, 215–233.

Poldrack, R.A., Halchenko, Y.O., Hanson, S.J., 2009. Decoding the large-scale structure of brain function by classifying mental states across individuals. Psychol. Sci. 20 (11), 1364–1372.

Price, C., 2009. The anatomy of language: A review of 100 fMRI studies published in 2009. Ann. N. Y. Acad. Sci. 1191, 62–88. https://doi.org/10.1111/j.1749-6632.2010.05444.x.

Redcay, E., Courchesne, E., 2008. Deviant functional magnetic resonance imaging patterns of brain activity to speech in 2-3-year-old children with autism spectrum disorder. Biol. Psychiatry 64 (7), 589–598. https://doi.org/10.1016/j.biopsych.2008.05.020.

Redcay, E., Moran, J.M., Mavros, P.L., Tager-Flusberg, H., Gabrieli, J.D.E., Whitfield-Gabrieli, S., 2013. Intrinsic functional network organization in high-functioning adolescents with autism spectrum disorder. Front. Hum. Neurosci. 7, 573. https://doi.org/10.3389/fnhum.2013.00573.

Rippon, G., Brock, J., Brown, C., Boucher, J., 2007. Disordered connectivity in the autistic brain: challenges for the "new psychophysiology". Int. J. Psychophysiol. 63, 164–172.

Rubinov, M., Sporns, O., 2010. Complex network measures of brain connectivity: uses and interpretations. Neuroimage 52, 1059–1069.

Rudie, J.D., Dapretto, M., 2017. Convergent evidence of brain overconnectivity in children with autism? Cell Rep. 5 (3), 565–566. https://doi.org/10.1016/j.celrep.2013.10.043.

Schmitz, N., Rubia, K., van Amelsvoort, T., Daly, E., Smith, A., and Murphy, D. G. M. (2008). Neural correlates of reward in autism. *The* Br. J. Psychiatry, 192(1), 19-24. Retrieved from http://bjp.rcpsych.org/content/192/1/19.abstract

Scott-Van Zeeland, A.A., Dapretto, M., Ghahremani, D.G., Poldrack, R.A., Bookheimer, S.Y., 2010. Reward processing in autism. Autism Res. 3 (2), 53–67. https://doi.org/10.1002/aur.122.

Smith, S.M., 2012. The future of fMRI connectivity. Neuroimage 62, 1257–1266.

Smith, S.M., Jenkinson, M., Woolrich, M.W., Beckmann, C.F., Behrens, T.E.J., Johansen-Bern, H., Bannister, P.R., De Luca, M., Drobnjak, I., Flitney, D.E., Niazy, R.K., Saunders, J., Vickers, J., Zhang, Y., De Stefano, N., Brady, J.M., Matthews, P.M., 2004. Advances in functional and structural MR image analysis and implementation as FSL. Neuroimage 23 (S1), 208–219.

Sporns, O., Betzel, R.F., 2016. Modular brain networks. Annu. Rev. Psychol. 672, 613–640.

Starck, T., Nikkinen, J., Rahko, J., Remes, J., Hurtig, T., Haapsamo, H., Jussila, K., Kuusikko-Gauffin, S., Mattila, M.L., Jansson-Verkasalo, E., Pauls, D.L., Ebeling, H., Moilanen, I., Tervonen, O., Kiviniemi, V.J., 2013. Resting state fMRI reveals a default mode dissociation between retrosplenial and medial prefrontal subnetworks in ASD despite motion scrubbing. Front. Hum. Neurosci. 7, 802. https://doi.org/10.3389/fnhum.2013.00802.

Stuart, M., McGrew, J.H., 2009. Caregiver burden after receiving a diagnosis of an autism spectrum disorder. Res. Autism Spect. Dis. 3 (1), 86–97.

Stufflebeam, S.M., Liu, H., Sepulcre, J., Tanaka, N., Buckner, R.L., Madsen, J.R., 2011. Localization of focal epileptic discharges using functional connectivity magnetic resonance imaging. J. Neurosurg. 114 (6), 1693–1697.

Sullivan, K., Stone, W.L., Dawson, G., 2014. Potential neural mechanisms underlying the effectiveness of early intervention for children with autism spectrum disorder. Res. Dev. Disabil. 35, 2921–2932.

Supekar, K., Uddin, L.Q., Prater, K., Amin, H., Greicius, M.D., Menon, V., 2010. Development of functional and structural connectivity within the default mode network in young children. Neuroimage 52 (1), 290–301. https://doi.org/10.1016/j.neuroimage.2010.04.009.

Sweet, A., Venkataraman, A., Stufflebeam, S.M., Liu, H., Tanaka, N., Golland, P., 2013. Detecting Epileptic Regions Based on Global Brain Connectivity Patterns. In: *MICCAI: Medical Image Computing and Computer Assisted Intervention*. Nagoya, Japan, LNCS, pp. 98–105.

Tononi, G., Sporns, O., Edelman, G.M., 1994. A measure for brain complexity: relating functional segregation and integration in the nervous system. PNAS 91, 5033–5037.

Tzourio-Mazoyer, N., Landeau, B., Papathanassiou, D., Crivello, F., Etard, O., Delcroix, N., Mazoyer, B., Joliot, M., 2002. Automated anatomical labeling of activations in {SPM} using a macroscopic anatomical parcellation of the {MNI MRI} single-subject brain. Neuroimage 15 (1), 273–289.

Van Dijk, K.R.A., Hedden, T., Venkataraman, A., Evans, K.C., Lazar, S.W., Buckner, R.L., 2010. Intrinsic functional connectivity as a tool for human connectomics: theory, properties, and optimization. J. Neurophysiol. 103 (1), 297–321.

Venkataraman, A., Van Dijk, K.R.A., Buckner, R.L., Golland, P., 2009. In: *Exploring Functional Connectivity in fMRI via Clustering*. *ICASSP: International Conference on Accoustics, Speech and Signal Processing*. IEEE, pp. 441–444.

Venkataraman, A., Kubicki, M., Westin, C.-F., Golland, P., 2010. In: *Robust Feature Selection in Resting-State fMRI Connectivity Based on Population Studies*. *MMBIA: IEEE Computer Society Workshop on Mathematical Methods in Biomedical Image Analysis*. IEEE, pp. 1–8.

Venkataraman, A., Kubicki, M., Golland, P., 2013a. From brain connectivity models to region labels: identifying foci of a neurological disorder. IEEE Trans. Med. Imaging 32 (11), 2078–2098.

Venkataraman, A., Kubicki, M., Golland, P., 2013b. From brain connectivity models to region labels: Identifying foci of a neurological disorder. IEEE Trans. Med. Imaging 32 (11), 697–704.

Venkataraman, A., Duncan, J.S., Yang, D., Pelphrey, K.A., 2015. An unbiased Bayesian approach to functional connectomics implicates social-communication networks in autism. NeuroImage Clin. 8, 356–366.

Venkataraman, A., Yang, D., Pelphrey, K.A., Duncan, J.S., 2016a. Bayesian community detection in the space of group-level functional differences. IEEE Trans. Med. Imaging 35 (8), 1866–1882.

Venkataraman, A., Yang, D.Y.-J., Dvornek, N., Staib, L.H., Duncan, J.S., Pelphrey, K.A., Ventola, P., 2016b. Pivotal response treatment prompts a functional rewiring of the brain among individuals with autism spectrum disorder. Neuroreport 1–5.

Venkataraman, A., Wymbs, N., Nebel, M., Mostofsky, S., 2017. In: *A Unified Bayesian Approach to Extract Network-Based Functional Differences from a Heterogeneous Patient Cohort*. *CNI: International Workshop on Connectomics in NeuroImaging*. Springer, pp. 1–8.

Waterhouse, L., Gilberg, C., 2014. Why autism must be taken apart. J. Autism Dev. Disord. 1–5. Retrieved from, https://doi.org/10.1007/s10803-013-2030-5.

Watson, R., Latinus, M., Charest, I., Crabbe, F., Belin, P., 2014. People-selectivity, audiovisual integration and heteromodality in the superior temporal sulcus. Cortex 50, 125–136. https://doi.org/10.1016/j.cortex.2013.07.011.

Wildgruber, D., Ackermann, H., Kreifelts, B., Ethofer, T., 2006. Cerebral processing of linguistic and emotional prosody: fMRI studies. Prog. Brain Res. 156, 249–268. https://doi.org/10.1016/j.neuroimage.2005.09.059.

Williams, J.H.G., Waiter, G.D., Perra, O., Perrett, D.I., Whiten, A., 2005. An fMRI study of joint attention experience. Neuroimage 25 (1), 133–140. https://doi.org/10.1016/j.neuroimage.2004.10.047.

Wolff, J.J., Gu, H., Gerig, G., Elison, J.T., Styner, M., Gouttard, S., Botteron, K.N., Dager, S.R., Dawson, G., Estes, A.M., Evans, A.C., Hazlett, H.C., Kostopoulos, P., RC, M.K., Paterson, S.J., Schultz, R.T., Zwaigenbaum, L., Piven, J., the IBIS Network, 2012. Differences in white matter fiber tract development present from 6 to 24 months in infants with autism. Am. J. Psychiatry 169, 589–600.

Xia, M., Wang, J., He, Y., 2013. BrainNet viewer: a network visualization tool for human brain connectomics. PLoS One 8, e68910. https://doi.org/10.1371/journal.pone.0068910.

Yang, D., Rosenblau, G., Keifer, C., Pelphrey, K.A., 2015. An integrative neural model of social perception, action observation, and theory of mind. Neurosci. Biobehav. Rev. 51, 263–275. Retrieved from, http://view.ncbi.nlm.nih.gov/pubmed/25660957.

Yarkoni, T., Poldrack, R.A., Nichols, T.E., Van Essen, D.C., Wager, T.D., 2011. Large-scale automated synthesis of human functional neuroimaging data. Nat. Methods 8, 665–670. https://doi.org/10.1038/nmeth.1635.